ISSN 0208-7774 TRIBOLOGIA 5/2018 p. 71–81

Anna PIĄTKOWSKA[*], Magdalena ROMANIEC[*], Danuta GRZYBEK[*], Małgorzata MOŻDŻONEK[*], Anna ROJEK[*],Ryszard DIDUSZKO[*]

A STUDY ON ANTIWEAR PROPERTIES OF GRAPHENE WATER-BASED LUBRICANT AND ITS CONTACT WITH METALLIC MATERIALS

BADANIA WŁAŚCIWOŚCI ANTYZUŻYCIOWYCH SMARU GRAFENOWEGO NA BAZIE WODY. KONTAKT SMARU Z MATERIAŁAMI METALICZNYMI

Keywords: graphene flakes, lubricant, friction, wear, oxidation.

Abstract

Due to their ecological and financial aspects, water-based lubricants may be competitive in use for production and sustainable technology. The paper presents tribological measurements results in the ball-flat friction node with reciprocal movement. The friction element manufactured of 316L stainless steel and 100Cr6 bearing steel cooperated under mixed friction with the use of water-based lubricants. Firstly, graphene flakes and graphite were applied as lubricant additives, both used as a similar reference material. Secondly, graphene lubricant reduced the friction coefficient and wear of friction elements. Interaction between water and graphene lubricants with 0.1 wt % and 1 wt % of graphene flakes and metal was also investigated. After 30 days of oxidation test in water and graphene lubricants, the Fe sample (Armco iron) surface was covered in graphene flakes with iron oxide structures. A compact coverage of the surface creates a protective layer against intensive oxidation in the distilled water-based graphene lubricant. The tests results have proven that the greater density of graphene flakes in the lubricant, the smaller is the amount of detected oxides. Graphene flakes agglomeration was observed in contact with the iron metal.

Słowa kluczowe: płatki grafenowe, smar, tarcie, zużycie, utlenianie.

Streszczenie

Ze względu na proekologiczny oraz finansowy aspekt smary na bazie wody mogą być konkurencyjne w zastosowaniu w produkcji i eksploatacji. W pracy przedstawiono wyniki badań tribologicznych w węźle tarcia kula–powierzchnia płaska w ruchu postępowo-zwrotnym. Elementy trące wykonane ze stali nierdzewnej 316L oraz łożyskowej 100Cr6 współpracowały w tarciu mieszanym z udziałem smaru na bazie wody. Jako dodatek zastosowano płatki grafenowe oraz grafit jako podobny materiał referencyjny. Smar grafenowy zmniejszył współczynnik tarcia oraz zużycie materiałów trących. Następnie zbadano oddziaływanie wody i smaru grafenowego 0,1%wt oraz 1%wt płatków grafenowych i metalu. Po 30 dniach kontaktu z próbką z żelaza Armco powierzchnia metalu pokryła się płatkami grafenowymi, na których wykrystalizowały tlenki żelaza. Przy zwartym pokryciu powierzchni uzyskano warstwę zabezpieczającą przed intensywnym utlenianiem w wodzie destylowanej, która stanowiła bazę smaru. Stwierdzono, że im większa zwartość płatków grafenowych w smarze, tym mniejsza ilość detektowanych tlenków. Zaobserwowano aglomerację płatków grafenowych w kontakcie z materiałem żelaza.

INTRODUCTION

Ten years have passed since graphene discovery. The prestigious discovery was appreciated, and received the Nobel Prize in Physics. Andre Gaim and Konstantin Novoselov, graphene inventors, who were awarded the Nobel Prize, isolated and discovered graphene properties: a one-atom carbon films. The new material has attracted attention of scientists. At that time, graphene was obtained through various methods. As a result, different technologies allowed extracting graphene in various forms: as a layer on a surface, or as

[*] Institute of Electronic Materials Technology, ul. Wólczyńska 133, 01-919 Warsaw, Poland, e-mail: Anna Piatkowska@itme.edu.pl.

a flake. Both forms have different properties and their potential usage is directed towards different production and exploitation areas.

The article describes graphene flake. As a physical definition of the material, it is not an ideal homogenous and chemically pure hexagonal structured carbon layer. Due to its manufacturing processes, the extracted chemically graphene flake consists of two-dimensional carbon structures with added atoms of oxygen and other element particles that are by-products of manufacturing process. The specific name of the material is graphene oxide, GO; or, as manufactured with reduction of oxygen – reduced graphene oxide, rGO. Their characteristics – especially chemical – are also different and may influence their potential usage.

Other important characteristics of the single graphene flake are size, morphology, and bundle size. The Institute of Electronic Materials Technology manufactures chemically graphene flakes that differ in size from several to single micrometres. Morphologically, the bigger graphene flakes have a more developed structure than the smaller ones. This results in different flake dispersion both in composites and in a liquid solution. There are many developed methods of graphene flakes manufacturing processes that allow undertaking effective methods for this material.

Two graphene properties have captured the attention of scientists regarding the tribology studies because of a high friction resistance of several hundred MPa and the well-known and profitable lubrication properties of carbon materials such as graphite.

Tribological properties of graphene were tested in nanoscale and microscale. The tip of an AFM microscope was used for nanotest, and millimetre-size balls were used as a counter specimen for micro-wear tests. The graphene was introduced into a friction pair as a component of a material composite, as a single or multi-layer coating, and finally as an additive to lubricants [**L. 1**]. In the review from 2014, the authors described the results that led to the general conclusion that graphene insertion into the friction pair always minimizes friction coefficients and wear.

For a mass scale application in regard to the tribological and financial aspects, the most useful is to manufacture the lubricant with graphene flakes. As the authors have proven, determining the optimal accumulation of graphene flakes required for optimal properties of a friction node depends on pressure, sliding speed, and a friction system geometry arrangement [**L. 3, 4**]. In comparison to standard referential lubricants, graphene lubricant practically always has better anti-wear and abrasive properties. Even though water is used as a lubricant base component [**L. 5, 6**], the coefficient of friction between the components is reduced two times in comparison to the application of a referential lubricant.

Using water as a base component for a lubricant in a metallic friction pair may seem to be a risky solution due to a possibility of a higher oxidizing level that worsens the tribological properties. However, the tests described above do not indicate that the metallic surfaces have a higher risk of corrosion during friction with the use of a graphene water-based lubricant. The effect was not observed, because the friction tests and contact with the water-based lubricant were not conducted longer than one hour. The anti-corrosion effect of graphene layers is well known and is conducted with the use of several percentage NaCl solutions [**L. 7, 8**].

The paper presents tribological test results with the use of a graphene water-based lubricant. The tribological friction pair aspects for steel-to-steel with the use of graphene lubricant are analysed together with distilled water and graphite mixture (another name is graphite lubricant). The friction coefficient and wear were measured, analysed, and described with the EDS method for measuring oxygen value in the friction area.

In order to determine the performance of graphene water-based lubricant on metallic elements that have contact with the lubricant without friction, oxidizing tests were conducted on the Armco alloy Fe sample.

The presented results are significant for the use of graphene water-based lubricant within metallic friction nodes. The results will also be important during a construction process for elements that have contact with graphene lubricant.

The offered research on water-based lubricants has a high environment-friendly significance, because it is not only linked to important taglines. Securing and recycling costs of oil products are increasing, [**L. 9**] which means that an introduction of new less environmentally aggressive products can contribute to lower expenses of manufacturing and devices exploitation.

MEASUREMENT METHOD

Material

Friction tests were conducted on a stainless steel 316L sample, and bearing steel 100Cr6 balls were used as a counter-specimen.

For the friction research, graphene water-based lubricant was applied containing 0.1 wt % of graphene flakes, distilled water mixture, and 1 wt % of graphite.

The tests regarding graphene flakes influence on oxidizing process for iron were performed and graphene water-based lubricant was used with the addition of the 0.1 wt % and the 1 wt % of graphene flakes.

Tribological tests

Friction tests were undertaken with the use of a DUCOM tribotester with the ‘ball-flat-ball’ friction node and with lineal and reciprocal movement of friction elements.

The friction test parameters were as follows:

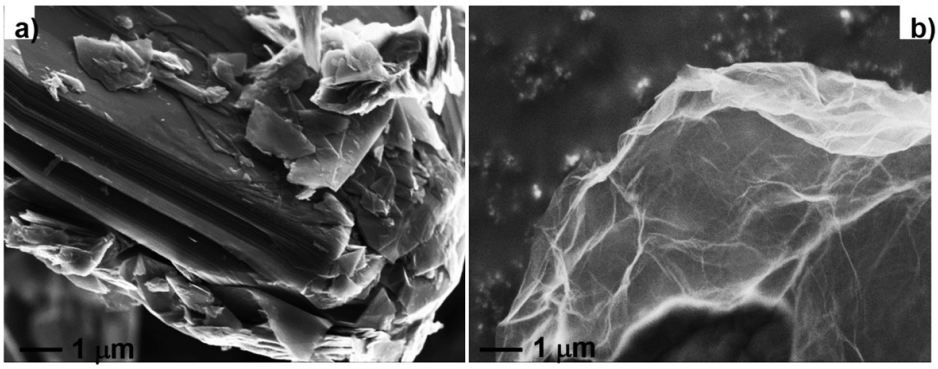

Fig. 1. SEM images of a) graphite, b) graphene flakes applied to water-based lubricants
Rys. 1. Zdjęcia mikroskopowe a) grafitu, b) płatków grafenowych zastosowanych jako dodatków do smarów na bazie wody

- Ball diameter (counter specimen) = ϕ 6,5 mm, of the bearing steel 100Cr6
- Load F = 10 N
- Sliding velocity v_s = 0.01 m/s
- Sliding distance = 9 m and 36 m
- Maximum contact point pressure calculated from Hertz equation p_{max} = ~1,3 GPa that is an optimal value for mobile shear force of graphene flakes.

Topography of friction traces, chemical composition

Microscopic measurements were performed with a Zeiss Auriga scanning electron microscope equipped with a Bruker X-Ray detector for Energy Dispersive X-ray spectroscopy (EDS) measurements. After oxidizing tests were performed, oxygen content analysis was made on the friction traces and on the surfaces of Armco alloy-samples. It was undertaken with the series of decomposition maps for oxygen chemical elements on the three areas that measured 0.03 mm^2 (with magnification of × 500). Micro-diameter cross-sections were performed with the ion-etched method with gallium ion by the Focused Ion Beam (FIB) system in which an Auriga Zeiss microscope is equipped. Before the ion milling process was performed, the friction surface was covered with platinum in order to avoid any damage. This action was performed with the use of a Gas Injected System.

Topographical measurements of friction traces were performed with the use of a 3D Bruker optical profiler. The measurements were made in the middle on the friction trace area of 1 mm^2. The friction traces were analysed on the fragments with the maximum depth on the measurement surface.

Fourier Transform Infrared Spectroscopy analysis (FTIR) – structural research

Structural surface tests were conducted with the use of Vertex 80v research spectrometer equipped with a platinum diamond ATR, which is a single reflection diamond crystal. Absorption spectrums were measured with the spectral range from 5500 to 400 cm^{-1}, and with the resolution of 2 cm^{-1}.

TEST RESULTS

Tribological test results

Friction tests were performed three times for all lubricant types and in the two friction variants that varied in duration of time. The friction temporary strength value F_t was measured during the test with the calibrated piezoelectric sensor. The conducted changes in the μ ratio were derived from the following equation:

$$\mu = F_t/F_n,$$

where F_n is load force, and F_t is measured friction force.

The results are described in **Fig. 2**.

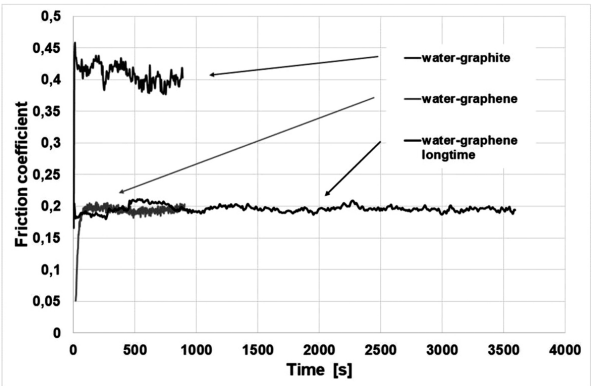

Fig. 2. Typical changes of friction coefficient in dependence of the type of lubricant
Rys. 2. Typowe zmiany współczynnika tarcia w zależności od rodzaju smaru

Figure 2 shows the results of friction tests of 15 min. and 60 min for the use of graphene lubricant. As a result, a very good repeatability of the coefficient of friction movement changes was received. The average coefficient of friction value with graphene-lubricant was 0.2±0.02, an the use of graphite lubricant resulted in an average coefficient of friction value of 0.45±0.1 coefficient of friction. It is visible in **Fig. 2**, where temporary changes in the coefficient of friction value were greater for graphite lubricant than for graphene lubricant. The long-term test of graphene lubricant resulted in a more stable coefficient of friction values. After two minutes of the test, stabilization of the coefficient of friction value resumed, and it remained on the same level until the end of the test.

During the tribological test part, both the ball and surface were submerged in lubricants at the point of contact. The friction type between the surfaces was mixed. **Fig. 3** shows the scope of microscopic results for the geometry and topographic measurements of friction movements that were presented in **Fig. 2**.

Regardless of the lubricant types used in the tests, the widths of traces are similar and are equal to ~300 μm. The difference lies within their shape and depth. The three-dimensional image and diagonal profile of wear traces with graphite lubricant show irregular topography with high edges and many micro scratches. The SEM images (**Fig. 3a**) show huge clusters of graphite. The clusters are chaotic assemblies of graphite bundles that are worn out during every move of a friction ball. The shape of the friction movement with graphene lubricant is symmetrical and regular in its shape with visible longitudinal scratches that came from the micro scratches.

With the use of graphite lubricant, the depth of wear trace is less in depth than the one that resulted during the friction process with graphite lubricant. Even after the long-term testing, the trace is shallower than the one achieved with graphite lubricant. It was observed that lengthening the duration of friction time does not lead to a substantial increase in the depth of the wear trace. After 15 minutes of friction, its depth was around 2.5 μm and after 60 minutes it was around 3 μm. Graphene flakes form clusters on the wear traces surface – especially in the middle part of the surface, as is visible in the **Figs. 3b** and **c**. Graphene clusters form a flat and uninterrupted band. The SEM images are taken with low current of electrons that allow determining very thin objects on the surface. The grey scale images allow evaluating the thickness of graphene flakes.

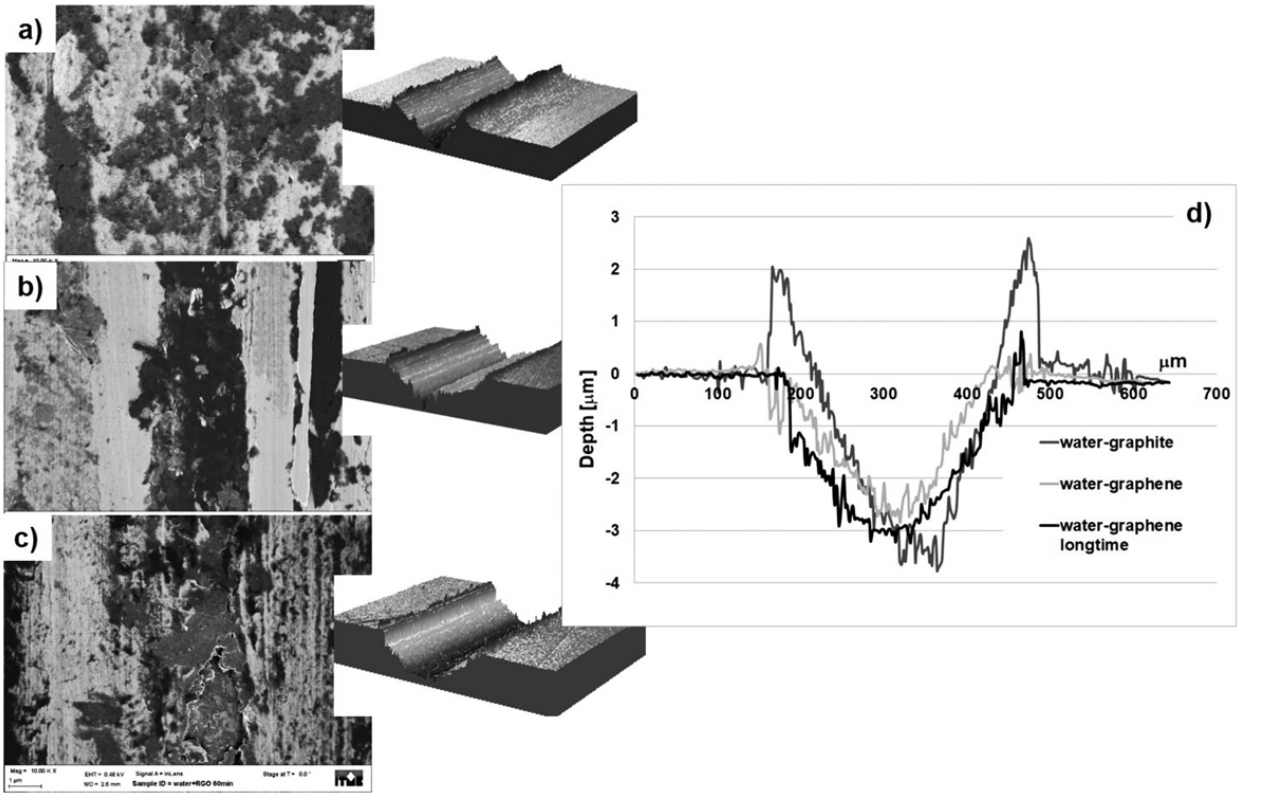

Fig. 3. Geometry and topography of the wear traces: SEM three-dimensional topography images of the wear part: a) with graphite lubricant, b) graphene lubricant after 15 min. of friction, c) graphene lubricant after 60 min. friction, d) cross-section of wear traces; arrows indicate direction of friction

Rys. 3. Geometria i topografia śladów tarcia. Zdjęcia SEM wraz z trójwymiarowymi obrazami fragmentu śladów tarcia: a) ze smarem grafitowym, b) ze smarem grafenowym po 15 min. tarcia, c) ze smarem grafenowym po 60 min. tarcia, d) profile poprzeczne śladów tarcia, strzałkami zaznaczono kierunek ruchu

The very small single graphene flakes are visible on the left side of **Fig. 3b**, and on the right side the stripe of amorphous carbon is visible. The scratches are shown as lighter lines that can be described as metallic surfaces with the use of mass contrast. The small torn flakes are visible on the surface after the long-term friction test. Mass contrast on the SEM images does not indicate the presence of the metallic surfaces on friction traces. The friction trace is wholly covered in graphene with various stages of damage.

The differences in tribological tests are a consequence derived from the type and properties of used lubricants. Graphite has hydrophobic properties. Even though the mixture of water and graphite seemed to be a homogeneous liquid, graphite bundles remained accumulated. The whole graphite bundles settled on the friction surface leading to additional resistance to movement. On the contrary, graphene lubricant is characterized in higher dispersion of graphene flakes. Water particles migrated among the single graphene layers in the flake separating it. Graphene lubricant was a mixture of liquid and floating separate and single graphene flakes. During the contact of friction surfaces, it was possible that that a separation of metallic surfaces was going to occur because of the graphene flakes, due to the fact that graphene flakes appeared on the surface or freely settled on the surface during immersion in graphene lubricant.

Unfortunately, the legendary graphene endurance was not confirmed during shear in contact with the micro roughness. The microscope observations confirm that most of the flakes are damaged during contact with an uneven surface. The undertaken tests show a dominance of the abrasive wear mechanism. The torn particles of metallic surfaces are partially removed from the friction area due to the material transfer process and the repeated press of this material into the friction area.

Another aspect of tests was to examine properties of the structural deformation of the subsurface of the wear trace. In order to obtain real and not deformed trace diameter by the cross-section of the trace, the micro-cuts were made with the use of ion etching with the FIB method. The SEM images reveal the formation of a tribofilm consisting of ground grains of alloy components of steel on the surface of traces.

The measured thickness on diameters of tribofilm is about 500 nm, and it does not depend on the duration of the friction test.

Figure 4 shows visible numerous additions (graphite and graphene), located between the metallic grains of the subsurfaces. Graphite is formed as the big amorphous-shaped inclusions. On the contrary, graphene forms the flat flake-shaped structures located on the surface. It can be observed that many flakes are located parallel to the surface. The long friction test did not increase the thickness of the tribofilm, but more flakes were deposited under the surface and they are more intricate.

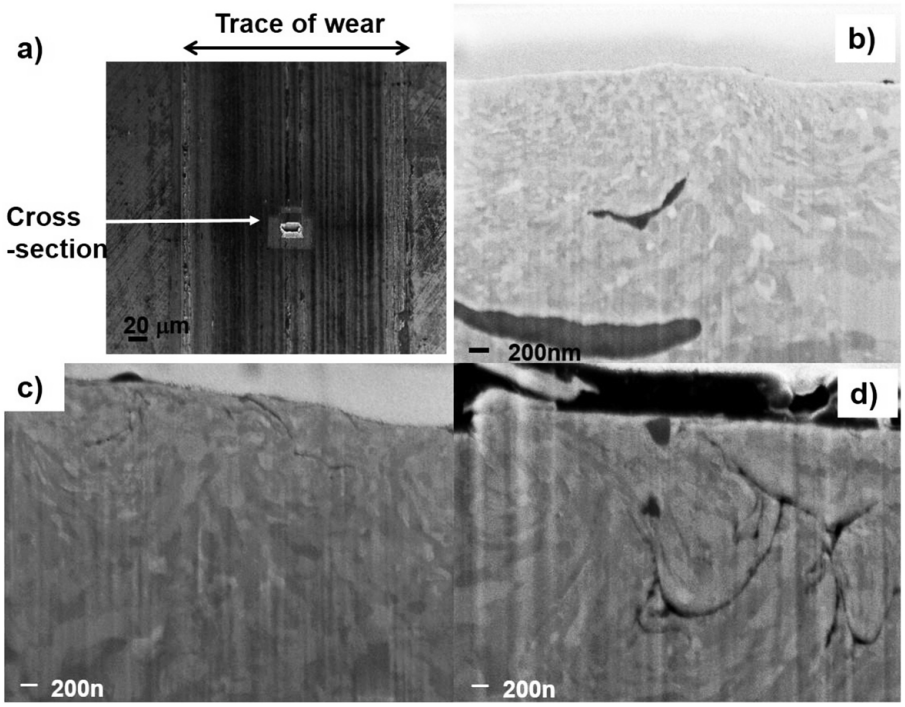

Fig. 4. SEM cross-section images of the wear traces: a) the location of the cross-section on the wear trace after friction with, b) graphite lubricant, c) graphene lubricant after 15 min. of friction, d) graphene lubricant after 60 min. of friction

Rys. 4. Zdjęcia SEM przekroju poprzecznego śladów tarcia: a) umiejscowienie przekroju po tarciu b) ze smarem grafitowym, c) ze smarem grafenowym 15 min., d) ze smarem grafenowym 60 min.

Due to the fact that the lubricants are water-based and due to their corrosive aspects, further tests were undertaken in order to specify and compare the oxidation intensity on the friction traces with the use of graphite and graphene lubricants. The EDS method was used to map the distribution of the Fe elements in the middle of friction traces. **Fig. 5** shows examples of the mapped area.

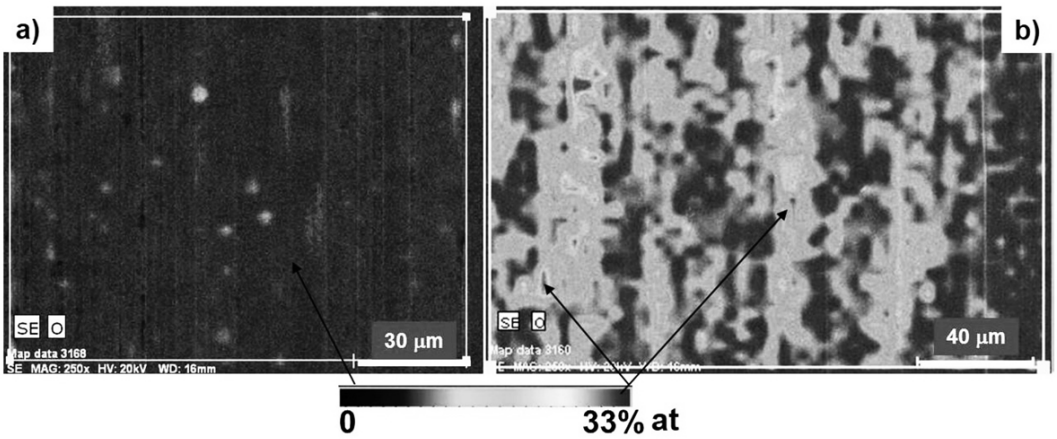

Fig. 5. The oxygen element distribution map on the wear traces after friction with: a) graphene lubricant, b) graphite lubricant; arrows indicated minimum and maximum the oxygen concentration

Rys. 5. Mapy intensywności rozkładu pierwiastka tlenu na śladach tarcia: a) ze smarem grafenowym, b) ze smarem grafitowym; strzałki wskazują skrajne koncentracje at. O

Due to the random choice of the EDS measurements, results may be locally non-representative. However, it may be generalized that graphene friction traces are less oxidized. The oxidized values found on the friction traces for graphene lubricant are expressed in the figures of 5% at, and for graphite lubricant the result is 8% at. In fact, the oxidized values for the metallic surface covered in graphene is lower due to the fact that the atom of oxygen is attached to the flakes.

Graphene flakes usage as an addition to the water-based lubricant turned out to have a positive influence, because the friction and wear value is lowered, which protected the metallic surfaces against higher level of oxidation.

The reason for these changes is the mechanism of easy slip of graphene flakes of their surface, obtaining a large dispersion of packets and flakes with water and good mechanical deposition of thin flakes on the surface protecting it against oxygen access and strengthening of the upper layer of material - tribofilm with very thin graphene flakes.

Graphene water-based lubricant can be potentially an eco-friendly equivalent for the standard lubricants and emulsions. The water-based lubricant had contact with the high quality steel specimens that have generally high anticorrosion properties. The short-term tests do not show the effective methods of the lubricant on the metallic parts.

Below, this article presents the results of oxidizing tests with the use of lubricant containing graphene flakes of 0.1 wt % and 1 wt %. In order to compare the influence of graphene flakes in distilled water, the results of oxidation of the Armco iron in distilled water will be presented.

After being polished and bathed in acetone and distilled water, the three Fe Armco samples were put in the tight flasks, as seen in **Fig. 6**.

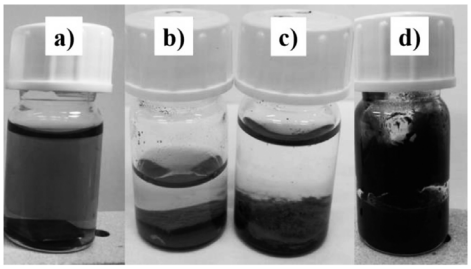

Fig. 6. Photos of the Fe samples in lubricants: a) graphene concentration of 0.1 wt % on the first day of test, b) distilled water after 30 days of the test, c) graphene concentration of 0.1 wt % after 30 days of the test, d) graphene concentration of 1 wt % after 30 day of the test

Rys. 6. Zdjęcia próbek Fe oraz smarów: a) grafenowy 0,1%wt w dniu rozpoczęcia testu, b) woda destylowana po 30 dniach, c) grafenowy 0,1%wt po 30 dniach, d) grafenowy 1%wt po 30 dniach

After several days, the oxidation process was visible as residual precipitates. A few hours were enough for graphene lubricant to undergo visible agglomeration and solid-fluid detachment. After 30 days, the Fe sample was covered with thick layer of oxides (**Fig. 6b**); however,

the contrary graphene lubricant of 0.1 wt % underwent complete delamination and the lubricant solidified. Before microscope observations of the surfaces of the oxidized Fe sample were performed, loose products of oxidation were removed and specimens were dried in argon atmosphere.

Visually surfaces of the Fe samples wetted in the pure water and lubricants had a matte finish and were covered with a fine coat layer. Microscopic observations revealed local non-homogeneous parts on the surface. Mild enlargement revealed visible residue "clusters," especially on the Fe sample immersed in distilled water, as in **Figs. 7a** and **c**.

More powerful magnification of the observed surface (**Figs. 7b** and **d**) revealed very complex crystallite structures. Shapes variety suggested the creation of various types of Fe oxides. It is important to mention that crystallites in the distilled water specimen were larger than the crystallites on the surface immersed in the graphene lubricant. The surface of the Fe sample wetted in graphene lubricant of 0.1 wt % was covered with graphene platelets, and the crystallites of Fe oxides were located mostly on the graphene surface. A fragment of pure graphene flake is visible in **Fig. 7d**. Many formed crystallites are visible on the right side. They are smaller than the ones visible in the distilled water specimen. Oxidizing in the lubricant of 1 wt % was a more expressive process, since, at the beginning, the fluid lubricant solidified and formed "a cork" that stuck to the surface of the Fe sample.

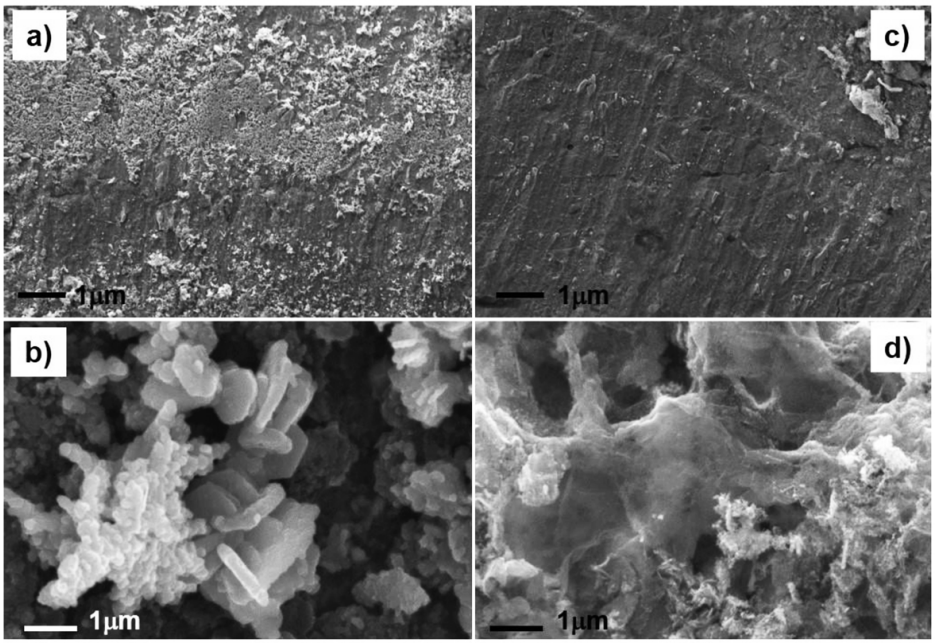

Fig. 7. SEM surface images of the Fe sample after 30 days of oxidation in water: a) magnification × 500, b) magnification × 10000, and in graphene lubricant of 0.1 wt %, c) magnification × 500, d) magnification × 10000

Rys. 7. Zdjęcia SEM powierzchni próbki Fe po 30 dniach utleniania w wodzie: a) powiększenie × 500, b) powiększenie × 10000, w smarze grafenowym 0.1 % wt, c) powiększenie × 500, d) powiększenie × 10000

"The cork," i.e. linked graphene flakes, could be easily removed and on the surface, and it was possible to distinguish two areas: Area 1 where the cork was bound to the surface, with a silvery colour, and Area 2 with a yellowish coating that did not adhere to the "cork." SEM images of both surfaces are presented in **Fig. 8**.

Differences between the two areas are mostly due to the number of formed crystallites.

In Area 1, crystallites were formed only on graphene platelets. The metallic surface is not covered, and is smooth. However, the flakes with crystallites cover all of Area 2.

The results of crystallites formation on graphene flakes are due to the process of the chemical reaction described in [**L. 11**], and this phenomenon may be used in water purification.

The "cork" formed on the surface consisted of packages of flakes separated by crystallites – a sandwich-like composite described in [**L. 13**] was obtained, resembling the arrangement of flakes with graphene paper.

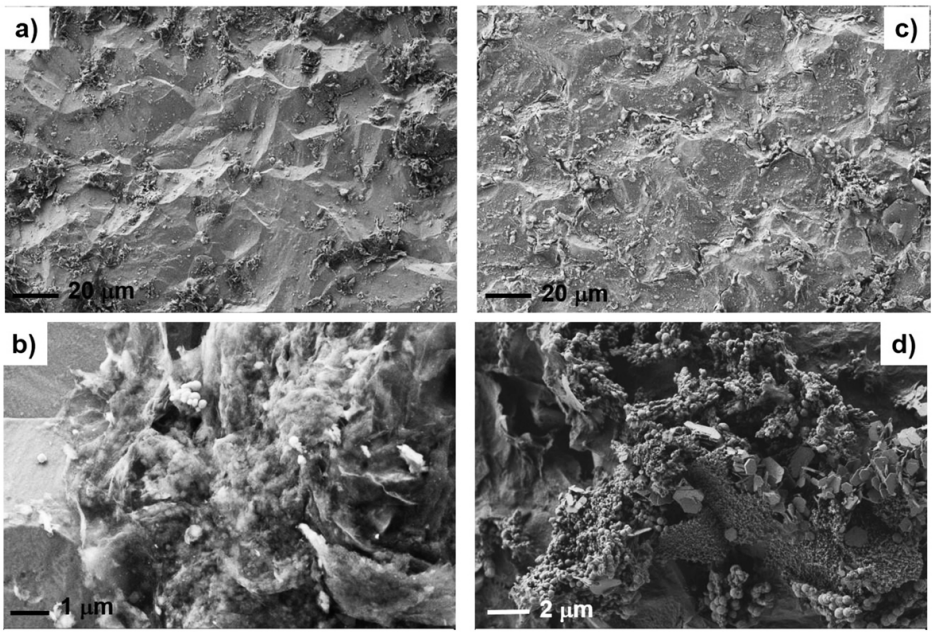

Fig. 8. SEM surface images of the Fe sample after 30 days of oxidation in graphene lubricant of 1 % wt.: Region 1 a) magnification × 500, b) magnification × 10000, Region 2, c) magnification × 500, d) magnification × 5000

Rys. 8. Zdjęcia SEM powierzchni próbki Fe po 30 dniach utleniania w smarze grafenowym 1%wt. Obszar 1: a) powiększenie × 500, b) powiększenie × 10000, w smarze grafenowym 1%wt. Obszar, 2 c) powiększenie × 500, d) powiększenie × 5000

Figure 9 presents the percentage measurements of the oxygen value in several areas that were the result of three oxidizing types of processes performed on the Fe samples.

Because EDS measurements were undertaken within three random areas, the specified percentage measurements (% at) of oxygen have different values, but one can see the following trend: The presence of

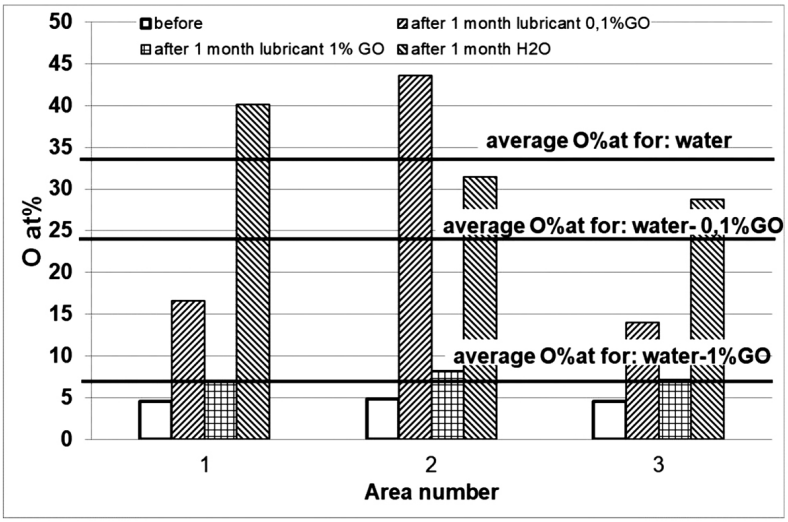

Fig. 9. EDS measurement summary of oxygen on the Fe surface samples before and after the oxidation tests in various lubricants

Rys. 9. Zestawienie pomiarów EDS zawartości tlenu na powierzchni próbek Fe przed i po procesach utleniania w różnych smarach

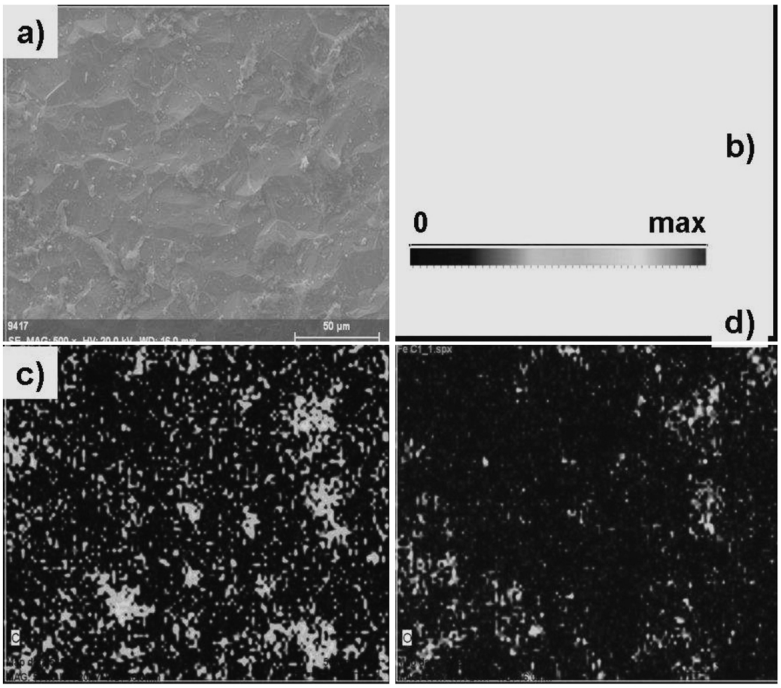

Fig. 10. EDS measurement results of the Fe surface sample after 30 days of oxidation test in graphene lubricant 1 wt %: a) SEM surface image, b) the qualitative amount scale % at., c) the carbon distribution map, d) the oxygen distribution map

Rys. 10. Zestawienie wyników pomiaru EDS z powierzchni próbki Fe utlenianej w smarze grafenowym 1%wt: a) zdjęcie SEM powierzchni badanego obszaru, b) skala zawartości detektowanych pierwiastków %at., c) mapa rozkładu węgla, d) mapa rozkładu tlenu

graphene in water reduces the amount of oxides formed as a result of Fe and H_2O reactions. In addition, it was observed that the higher the value of graphene flakes, the lower is the value of oxide detected on the Fe specimen surface.

Figure 10 shows carbon and oxygen distribution maps. SEM surface images and the map show that oxygen is mostly detected on the carbon objects, i.e. they adhere on the surface of graphene flakes.

The FTIR structural measurements allowed determining precisely the oxides type that formulated on the Fe specimen surface. **Fig. 11** presents measured absorption spectrums.

The FTIR measurements were undertaken within a few specimen areas due to the various colours of their surfaces that indicate the formation of different structures. For better spectrum visualizations, lines were moved towards the absorbance axis with no scale changes. Heights of spectrum peaks are equal to the amount of structure occurrence.

Waves are visible within spectrums and are characteristic for GO: C=O (1720 cm^{-1}), O-H z H_2O (1648 cm^{-1}), C=C with aromatic rings of sp^2 hybridized (1578, 1559, 1456 cm^{-1}), and C-O and C-O-C (the wavelength between 1250 and 1000 cm^{-1}). The wavelength location C=C with 1578 cm^{-1} in Spectrum 1 indicates on increased reduction of graphene oxidant. The presence of wavelength 603 and 470 cm^{-1} in Spectrum 4 indicates the presence of α-Fe_2O_3. The lines are broad and seemingly contain several absorbing lines that come from the different types of Fe oxides and hydroxides. However, the wavelength of 892, 801 and 747 cm^{-1} together with 1023 cm^{-1} indicate that O-H groups are present, i.e.the hydroxides of α-FeOOH, γ-FeOOH i β-FeOOH. The wavelength of 3700–2500 cm^{-1} frequency was also present, which is not visible in the figure, but is caused by vibrations of extending O-H groups. The broad wavelength of 569 cm^{-1} derived from the Fe_3O_4 particle is visible in Spectrum 5. The wavelength is complex due to its asymmetry and its two-humped shape, and it contains the wavelength from α-Fe_2O_3. Furthermore, the presence of α-Fe_2O_3 is linked to the 470 cm^{-1} wavelength.

On the Fe specimen surface immersed in distilled water, the Fe-oxides of Fe_2O_3 and a smaller amount of Fe_3O_4 are present. There are also the hydroxides of the Fe-OOH group detected. They are more frequent in presence than the Fe-oxides detected on the Fe specimen surface oxidized in the lubricant of 1%wt or even on "the cork" surface. The FTIR measurement results confirm the conclusions from the microscopic observation and EDS measurements. An interesting effect of the FTIR

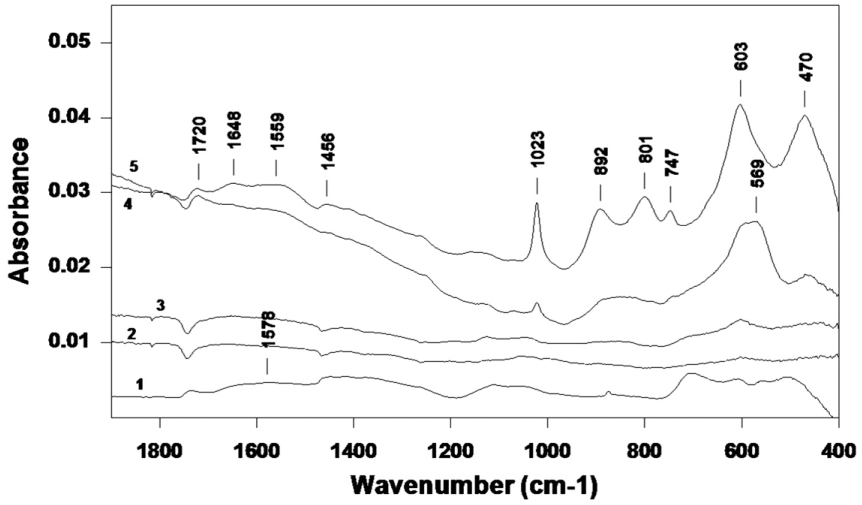

Fig. 11. Absorption spectrums of the Fe samples after oxidation in water and graphene lubricants with characteristic lines corresponding to iron oxides and graphene structures: 1 – The lubricant of 1 wt % after 30 days of the test and dehydration (sandwich-like-composite), 2 – The Fe sample after oxidation in graphene lubricant of 1 wt % – region 1, 3 – The Fe sample after oxidation in graphene lubricant of 1 wt % – region 2, 4, 5 – different areas of the Fe sample oxidized in water

Rys.11. Widma absorpcyjne próbek Fe utlenianych w wodzie i smarze grafenowym z charakterystycznymi liniami odpowiadającymi tlenkom żelaza oraz strukturom grafenowym: 1 – smar 1%wt po 30 dniach testu i wysuszeniu (sandwich-like kompozyt), 2 – próbka Fe po utlenianiu w smarze grafenowym 1%wt – obszar 1, 3 – próbka Fe po utlenianiu w smarze grafenowym 1%wt – obszar 2, 4, 5 – różne obszary próbki Fe utlenianej w wodzie

measurement is the finding of numerous occurrences of typical graphene structures, which, as a result of the addition of Fe-oxides crystallites, do not undergo significant deformation. The graphene reduction measured by the FTIR is the result of oxygen atoms removal from graphene flakes that allow creating more "pure" graphene.

CONCLUSIONS

The main objectives of the tests were to investigate the tribological properties and influence of graphene water-based lubricant on Fe samples. Tribological tests of graphene lubricant were compared to the tests results undertaken with presence of graphite lubricant, as a cheaper material that is similar to coal in origin and structure. The lubricants used in the tests differed in the concentration of the additive. The graphite lubricant was obtained by adding 1% wt of graphite flakes to deionized water. The graphene lubricant for friction tests was made with the addition of 0.1% wt graphene flakes.

As a result of the research, it was found that graphene lubricant reduces the coefficient of friction more than double, and it also reduces the wear of the friction pair compared to lubricant with the addition of graphite. The analysis of traces of friction also showed a significant reduction in the oxidation of the surface after friction tests involving graphene lubricant. It is important that, during long-term friction tests, the coefficient of friction was been stabilized and the wear increased very slightly. The better frictional properties of graphene lubricant are obtained partially due to the separation of graphene flakes in water into quasi-individual atomic layers. In addition, the tribofilm generated during friction contains embedded graphene flakes that can strengthen the structure and prevent intense damage. Graphene water-based lubricant properties predispose toward practical usage, especially with positive ecological tendencies.

Due to the fact that friction was applied on the high quality steel with anticorrosion properties, it is important to determine the influence of graphene water-based lubricant on the pure metallic materials. ARMCO iron samples (79% Fe) subjected to the oxidation process were tested for the comparison of the oxidation state of the Fe surface in contact with distilled water and graphene lubricants with different graphene content – 0.1%wt and 1%wt graphene.

It was demonstrated that the presence of graphene flakes decreases the creation of Fe oxides. Embedded graphene flakes on the metallic surface prevented it from intensive oxidizing. After the analysis of the results, it was concluded that, with a higher percentage amount of graphene addition in H_2O, the surface of the Fe-sample is more impermeably covered with graphene which leads to decreased oxidation. However, the oxidizing process takes place and formulated crystallites of mostly Fe_2O_3 can be found on graphene flakes. During the long-term influence of graphene water-based lubricant on alloy,

a thick graphene- Fe-oxide composite is created that decelerates the oxidizing process. Graphene lubricant delaminates, agglomerates, and loses its interesting lubricant properties in the contact with the metallic surface. Unfortunately, this characteristic can limit potential usage, and it imposes other solutions towards material-construction of the friction node.

REFERENCES

1. Berman D., Erdemir A., Sumant A.V.: Graphene: a new emerging lubricant. Materials Today. 2014, 17(1): 31–42.
2. Gupta B., Kumar N., Panda K., Dash S., Tyagi A.K.: Energy efficient reduced graphene oxide additives: mechanism of effective lubrication and antiwear properties. 2016, Scientific Reports/6:18372/DOI: 10.1038/srep18372: 1–10.
3. Senatore A., D'Agostino V., Petrone V., Ciambelli P., Sarno M.: Graphene oxide nanosheets as effective friction modifier for oil lubricant: materials, methods and tribological results. Tribology. 2013. Article ID 425809; http://dx.doi.org/10.5402/2013/425809.
4. Rasheed A.K., Khalid M., Rashimi W., Gupta T.C.S. M., Chan A.: Graphene based nanofluids and nanolubricants – review of recent developments, renewable and sustainable energy reviews. 2016(63): 346–362.
5. Liang S., Shen Z., Yi M., Liu L., Zhang X., Ma S.: In-situ exfoliated graphene for high-performance water-based lubricants carbon 2016(96): 1181–1190.
6. Elomaa O., Singh V.K., Iyer A., Hakala T.J., Koskinen J.: Graphene oxide in water lubrication on diamond-like carbon vs. stainless steel high-load contacts diamond and related material. 2015(52): 43–48.
7. Liang S., Shen Z., Yi M., Liu L., Zhang X., Ma S.: In-situ exfoliated graphene for high-performance water-based lubricants carbon 2016(96): 1181–1190.
8. Chaudry A.U., Mittal V., Mishra B., 2015. Effect of graphene oxide nanoplatelets on electrochemical properties of steel substrate in saline media, materials chemistry and physics 2015(163): 130–137.
9. http://www.recykling.pl/recykling/index.php/r/odpady/264/o/16
10. Spear J.C., Ewers B.W., Batteas J.D.: 2D-nanomaterials for Controlling Friction and Wear at Interfaces. Nao Today. 2015(10): 301–314.
11. Jin Kan, Yong Wang: Large and fast reversible storage li-ion storages in Fe2O3 graphene sheet-on-sheet sandwich-like compostes. 2013, Scientific Reports. 3:3502/DOI:10.1038/srep03502.
12. Hui Su, Zhibin Ye, Nuri Hmidi: High-performance iron oxide-graphene oxide nanocomposite adsorbents for arsenic removal, colloids and surfaces a: physicochem. eng. aspects. 2017(522): 161–172.
13. Liu Yu, Zhan Y., Ying Y., Peng X.: Fe_3O_4 nanoparticle anchored layered graphene films for high performance lithium storage. New J. Chem. 2016(40): 2649–2654.